Myocardial and Systemic Inflammation in Acute Stress-Induced (takotsubo) Cardiomyopathy

Caroline Scally, MBChB MRCP[1], **Hassan Abbas, MBChB MRCP**[1], **Trevor Ahearn, BSc, MSc, PhD**[1], **Janaki Srinivasan, RDCS, BSE**[1], **Alice Mezincescu, MD MRCP**[1], **Amelia Rudd, RDCS, BSE**[1], **Nicholas Spath, MBBS MRCP**[2], **Alim Yucel-Finn, MSc MBBS FRCR**[1], **Raif Yuecel, PhD**[1], **Keith Oldroyd, MBChB, MD(Hons), FRCP(Glasg), FESC**[3], **Ciprian Dospinescu, MD, MRCP PhD**[1], **Graham Horgan, BA, MSc, PhD**[4], **Paul Broadhurst, MBBS, MD, FRCP**[1], **Anke Henning, BSc, MSc, PhD**[5], **David E. Newby, PhD, DM, FACC, FESC**[2], **Scott Semple, BSc, MSc, PhD**[2], **Heather M. Wilson, BSc,PhD**[1], and **Dana K Dawson, MD, FRCP, D.Phil, FESC**[1]

[1]Aberdeen Cardiovascular and Diabetes Centre, University of Aberdeen, Aberdeen, United Kingdom

[2]BHF Centre for Cardiovascular Sciences, University of Edinburgh, Edinburgh, United Kingdom

[3]West of Scotland Regional Heart & Lung Centre, Glasgow, United Kingdom

[4]Biomathematics & Statistics Scotland, Aberdeen, United Kingdom

[5]University of Tubingen, Tubingen, Germany

Abstract

Background—Acute stress induced (takotsubo) cardiomyopathy can result in a heart failure phenotype with a prognosis comparable to myocardial infarction. In this study, we hypothesized that inflammation is central to the pathophysiology and natural history of takotsubo cardiomyopathy.

Methods—In a multi-centre study, we prospectively recruited 55 patients with takotsubo cardiomyopathy and 51 age, sex and co-morbidity matched control subjects. During the index event and at 5 months follow-up, patients with takotsubo cardiomyopathy underwent multiparametric cardiac magnetic resonance imaging including ultrasmall superparamagnetic particles of iron oxide (USPIO) enhancement for detection of inflammatory macrophages in the myocardium. Blood monocyte subpopulations and serum cytokines were assessed as measures of systemic inflammation. Matched controls underwent investigation at a single time point.

Results—Subjects were predominantly middle aged (64±14years) women (90%). When compared to control subjects, patients with takotsubo cardiomyopathy had greater USPIO enhancement (expressed as the difference between pre-USPIO and post-USPIO T2*) in both

ballooning (14.3±0.6 *versus* 10.5±0.9 ms, p<0.001) and non-ballooning (12.9±0.6 *versus* 10.5±0.9 ms, p=0.02) left ventricular myocardial segments. Serum interleukin-6 (23.1±4.5 *versus* 6.5±5.8 pg/mL, p< 0.001) and chemokine (C-X-C motif) ligand 1 (1903±168 *versus* 1272±177 pg/mL, p=0.01) concentrations, and classical $CD14^{++}CD16^-$ monocytes (90±0.5 *versus* 87±0.9%, p=0.01) were also increased whilst intermediate $CD14^{++}CD16^+$ (5.4±0.3 *versus* 6.9±0.6%, p=0.01) and non-classical $CD14^+CD16^{++}$ (2.7±0.3% *versus* 4.2±0.5%, p=0.006) monocytes were reduced in patients with takotsubo cardiomyopathy. At 5 months, USPIO enhancement was no longer detectable in the left ventricular myocardium although there remained persistent elevations in serum interleukin-6 concentrations (p=0.009) and reductions in intermediate $CD14^{++}CD16^+$ monocytes (5.6±0.4 *versus* 6.9±0.6%, p=0.01).

Conclusions—We demonstrate for the first time that takotsubo cardiomyopathy is characterized by a myocardial macrophage inflammatory infiltrate, changes in the distribution of monocyte subsets and an increase in systemic pro-inflammatory cytokines. Many of these changes persisted for at least 5 months suggesting a low-grade chronic inflammatory state.

Keywords

acute stress induced cardiomyopathy; takotsubo; inflammation; monocyte; macrophage; cytokines; ultrasmall superparamagnetic iron oxide particles (USPIO)

Introduction

Acute stress-induced (takotsubo) cardiomyopathy is a heart failure syndrome which has a similar presentation and mortality to acute myocardial infarction (MI)1–3. Often triggered by a major stressful event, these patients have unobstructed coronary arteries and characteristic ballooning of the left ventricle, with subsequent prompt restoration of normal or near normal ejection fraction. However, we have recently shown that despite previous preconceptions, takotsubo cardiomyopathy results in a long-term heart failure phenotype with persistent symptoms and subclinical cardiac dysfunction4. We and others have also shown global severe edema of both the left and right ventricular myocardium that does not completely resolve by 4 months after the acute event despite spontaneous normalization of the ejection fraction5–8. Given the persistence of myocardial tissue edema and heart failure symptoms, we hypothesized that the pathophysiology of takotsubo cardiomyopathy may relate to prolonged activation of cellular and humoral inflammatory pathways. Our aim was to investigate whether there is evidence of acute localized macrophage-mediated inflammation within the myocardium (primary end-point) with or without evidence of systemic inflammation by assessing monocyte sub-populations and serum cytokine concentrations. Furthermore, we wished to explore the time course and persistence of any of these potential pro-inflammatory pathways.

Methods

Study design

This was a multi-centre, prospective, case-control, mechanistic investigation.

Study population

Fifty-five patients with acute takotsubo cardiomyopathy were recruited from five Scottish cardiac centres (Aberdeen, Dundee, Edinburgh, Glasgow and Inverness). All patients had invasive coronary angiography and left ventriculography at the time of the diagnosis, and they fulfilled the Mayo Clinic9 and the European Society of Cardiology - Heart Failure Association diagnostic criteria for takotsubo cardiomyopathy10 – specifically they had typical left ventricular ballooning (apical, mid-cavity or basal), normal or near normal coronary arteries without any evidence of obstructive or culprit coronary plaque, developed QTc prolongation 24-48 hours after presentation and had modest cardiac biomarker release. A stressful trigger was identified in the majority (examples shown in Supplemental Table 1) and finally the recovery of left ventricular ejection fraction to normal values seen at follow-up confirmed the initial takotsubo diagnosis. Exclusion criteria were any acute or chronic infectious diseases or other inflammatory conditions such as flu-like illness, upper or lower respiratory tract infection, gastro-enteritis, urinary tract infection, any pyrexial illness or septic presentation, asthma, eczema, allergy, rheumatoid arthritis, systemic lupus erythematosus, Crohns' disease, ulcerative colitis (list not exhaustive), or any concurrent physical illness that in the judgement of investigators was a potential confounder to the hypothesis (e.g. concurrent hypertrophic or non-compaction cardiomyopathy, moderate to severe left ventricular hypertrophy of any cause), known allergies or intolerance to intravenous iron compounds and contraindications to magnetic resonance scanning. In particular acute pericarditis and acute myocarditis were carefully excluded both on clinical and imaging grounds (presenting history, absence of stressful trigger, ECGs, distribution of wall motion abnormalities with no ballooning and when seen, presence of late gadolinium enhancement pattern suggestive of myocarditis). One patient died after hospital discharge and an additional 6 did not wish to return for follow-up. Age, sex and co-morbidity matched control subjects (n=51) from the University of Aberdeen volunteer database were invited to participate. In order to match the co-morbidities of the takotsubo participants precisely, control subjects were chosen to be (i) healthy and on no medication, (ii) have isolated hypertension on one antihypertensive medication only, or (iii) have diabetes mellitus (diet or metformin controlled).

Study Protocol

The study was approved by the Institutional Review Board and Research Ethics Committee, and all subjects gave written informed consent. Patients underwent prompt assessment (within 14 days) after the onset of takotsubo cardiomyopathy which was repeated 5 months after the index event. Study assessments included blood sampling, two-dimensional and Doppler echocardiography, and multiparametric cardiac magnetic resonance. The latter also included cardiac ^{31}P-spectroscopy, late gadolinium enhancement and repeated scanning exactly 24 hours after intravenous infusion of ultrasmall superparamagnetic particles of iron oxide (USPIO) (ferumoxytol, AMAG Pharmaceuticals, Waltham, MA, USA), as described previously for tracking phagocytic macrophages11 including those in the myocardium of patients with acute myocardial infarction11–13. At the 5-month follow-up visit, all patients underwent repeated study assessments as well as an assessment of symptom burden including New York Heart Association (NYHA) and Minnesota Living with Heart Failure Questionnaire (MLHFQ).

Blood sampling was performed during the acute phase (days 0-13 from acute onset) and at 5 months follow-up.

Cardiovascular biomarkers and inflammatory cytokines

Blood was clotted, and serum separated by centrifugation at 50 g for 10 min and stored at -80°C until cytokine analysis. Brain natriuretic peptide (BNP) concentrations were determined using an immunoassay (Alere Triage MeterPro; Delaware, USA). High-sensitivity troponin I (ARCHITECT$_{STAT}$, Abbott Laboratories, Abbott Park, IL, USA) was obtained at follow-up in addition to the routine 12-hour clinical troponin from admission. Clinical hematology and biochemistry was performed as part of clinical care. Quantification of serum cytokine concentrations - chemokine (C-X-C motif) ligand 1 (CXCL-1) - or growth regulated protein (GROα), tumour necrosis factor alpha (TNF-α), interferon gamma (IFN-γ), monocyte chemoattractant protein 1 (MCP-1) and the interleukins (IL-1β, IL-6, IL-8 (CXCL8), IL-10, IL-12p40) - were performed using a bespoke commercially available human multiplex cytokine kit (MILLIPLEX MAP Human Cytokine/Chemokine Magnetic Bead Panel, catalogue #HCYTOMAG-60K-09, Merck Millipore, Darmstadt, Germany).

Monocyte Phenotyping

Percentages of monocyte subsets were measured from venous blood using a BD LSR Fortessa flow cytometer and analysed using FlowJo version 10. Anti-human antibodies CD45 V450 (clone HI30), CD14 PE-CF594 (clone MφP9), CD16 PE-Cy7 (clone 3G8) and HLA-DR FITC (clone G46-6) were mixed with 100 μL fresh EDTA anti-coagulated blood. After 20 minutes of incubation in the dark, red blood cells were lysed and fixed using FACSlyse (BD) for 20 minutes followed by dilution in 2 mL p*hosphate-buffered* saline (PBS) solution and after a final washing step, cells were re-suspended in 0.5 mL PBS and subjected to immediate flow cytometric analysis. To identify monocytes, first forward scatter (FSC) and side scatter (SSC) were used to identify cells from debris, then cells were visualized in a SSC/CD45 plot to gate on a monocyte population. CD45+/HLA-DR positive cells were gated to exclude any CD16^{+} natural killer cells and other non-MHC expressing cells. Unstained, Fluorescence Minus One (FMO) and internal controls were used for setting the boundaries of the gates. Monocyte subpopulations were identified from a CD14 *versus* CD16 bi-variate plot following the criteria defined previously[14] as three monocyte sub-populations: CD14^{++}CD16^{-} (classical, pro-inflammatory), CD14^{++}CD16^{+} (intermediate) and CD14^{+}CD16^{++} (non-classical).

Ex-vivo Monocyte-Macrophage Differentiation

CD14^{+} peripheral blood monocytes were isolated from whole blood from 5 female patients with acute takotsubo cardiomyopathy (upon presentation) and 5 female healthy control subjects, and each incubated in their autologous serum for 7 days to induce differentiation into macrophages. USPIO (ferumoxytol) was added to the macrophages for 24 hours with final concentrations of 0 (control), 40 and 80 μg/mL. Total iron in cell lysate was quantified colorimetrically using a validated 2,2'-bipyridine assay measuring absorbance at 520 nm. The mean iron of triplicate wells for each USPIO concentration was expressed as ng/μg protein.

Transthoracic Echocardiography

Echocardiography was performed using Vivid E9 systems, equipped with 2.5 MHz (M5S) transducers (GE Vingmed, Norway) and analysed by a single experienced British Society of Echocardiography-accredited sonographer. Three cardiac cycles in each of the standard parasternal long axis, short axis, apical 4, 3 and 2-chamber views were obtained at end-expiratory breath-hold at a frame rate of at least 85 Hz and stored for off-line analysis. Any subject with left bundle branch block (LBBB) on ECG was excluded from the strain and deformation analysis. Image analysis was performed using EchoPAC software (Version 1.13, GE Healthcare) as previously described measuring left ventricular longitudinal, radial and circumferential strain and deformation indices[15].

[31]P Cardiac-Magnetic Resonance Spectroscopy (^{31}P-CMRS) and Cardiac Magnetic Resonance Imaging (CMR)

All participants were scanned on either 3T Philips Achieva TX (Aberdeen) or 3T Siemens Verio (Edinburgh): 48 patients were scanned in Aberdeen and 7 in Edinburgh; all matched controls were scanned in Aberdeen. All sequences were validated in Aberdeen and an effort has been made to ensure similar parameters between scanners. ^{31}P-CMRS was acquired using a 14-cm diameter transmit and receive ^{31}P surface coil as described previously[5] (only patients scanned in Aberdeen underwent ^{31}P-CMRS, n=48). A non-water-suppressed ^{1}H point resolved spectroscopy acquisition was used to monitor resonance frequency determination and B_0 shimming over the ^{31}P-CMRS volume of interest, which was positioned to cover the entire inter-ventricular septum. The ^{31}P-CMRS acquisition was an ECG-gated image selected *in vivo* spectroscopy sequence, triggered to mid-late diastole, with a repetition time of at least 10 seconds.

A 6-channel cardiac coil (Philips) or a 32-channel cardiac array coil (Siemens) was used to acquire cine imaging, whole left ventricle pre-contrast T1 mapping (5s(3s)3s scheme), whole left ventricle multi-echo gradient echo T2* sequence (TE's of 1.15, 2.15, 3.15, 4.15, 5.15, 6.15, 7.15, 8.15, 9.15 and 10.15 ms), early and late gadolinium enhancement (Gadovist, 0.1 mmol/kg) with swap of the phase-encoding direction and *exactly 24 hour* post-USPIO acquisition of whole left ventricle multi-echo gradient echo T2*. The USPIO (ferumoxytol 4mg/kg in 50 mL of 0.9% saline) was administered as an intravenous infusion over 30 minutes following baseline cardiac magnetic resonance. All left ventricular imaging was performed with a slice thickness of 10 mm.

Image Analysis

^{31}P-CMRS data were analysed in JMRUi3.0 as described previously[5]. The phosphocreatine/γ-adenosine triphosphate (PCr/γATP) ratio (which is the gold standard for *in-vivo* assessment of myocardial energetic status[16]) was determined after the γ-ATP was corrected for blood contamination and PCr/γATP ratios were saturation-corrected as described previously[17–19]. To ensure that spectra were of good quality, Cramér-Rao standard deviations of all peaks were calculated and only those <20% were accepted. T2* and T1 maps were analysed in each of the 16 segments of the 17-segment model[20] (omitting the true apex) using CMR Tools (Cardiovascular Imaging Solutions, London, UK) and Segment (Medviso, Lund, Sweden), respectively. T2* values were generated for each of the 16

segments from native images before and 24 hours after ferumoxytol. The post-ferumoxytol values were subtracted from the native values in each segment to derive the <u>change in T2*</u> as a measure of ferumoxytol uptake by tissue resident macrophages11. Left ventricular volumes, mass and ejection fraction were calculated in CMR Tools. Each segment of the heart was given a wall motion score (1=normal, 2= hypokinesia, 3=akinesia and 4= dyskinesia); any segment with a score of >1 was assigned as ballooning and any segment with a score of 1 was assigned as non-ballooning. Imaging data are reported grouped by wall motion (ballooning and non-ballooning), by left ventricular region (apex, mid-cavity or base) and for the whole left ventricle.

Our inter-observer variabilities for strain echocardiography, ^{31}P-CMRS and CMR have been reported previously and ranged between 3-6±1-2% for all strain echocardiography parameters, 1.5-2.7±0.5-1.5% for cardiac magnetic resonance inclusive of T1 mapping and 5±2% for PCr/γATP ratio5,6,15. Inter-observer variability for T2* measurements were 5.4±3%.

The data, analytic methods, and study materials will be made available to other researchers for purposes of reproducing or replicating these findings.

Statistical Analysis

The main study outcome was myocardial inflammation assessed by the change in T2* from native to post-USPIO images and the secondary outcome was the presence of systemic inflammation assessed from changes in monocyte sub-populations and serum cytokine concentrations. Data were analysed by a mixed model with random effects for patient and fixed effects for subject group, with age and gender as covariates, followed by post-hoc comparisons of subject groups or time-intervals; p-values for comparisons were calculated using t-tests with degrees of freedom estimated by the Satterthwaite method. Tabulated data are shown as mean ± SEM or median (range). Statistical significance was set at $p < 0.05$.

Results

Fifty-five patients presenting with acute takotsubo cardiomyopathy were recruited and assessed at baseline, and 48 were re-studied at a mean of 148±7 days following their index event. They were predominantly middle aged or elderly (median 64 years, range 28-83) women (n=50 (91%)). Their characteristics are summarized in Table 1. Fifty-one control subjects were well matched with a comparable age (median 63 years, range 38-85), gender (46 women, 90%) and co-morbidity distribution.

Myocardial Inflammation Assessed with USPIO-Enhanced Cardiac Magnetic Resonance

There was a higher <u>change</u> in T2* values in both the ballooning and the non-ballooning segments of patients with acute takotsubo cardiomyopathy compared to control subjects (p=0.002 and p=0.02, respectively) (Table 2, Figure 1), indicating an increase in myocardial macrophages. Results were similar when analysed by left ventricular region, with the apex and mid-cavity demonstrating changes compared to control subjects (p<0.01 for both). After 5 months, the post-USPIO change in T2* was comparable to that seen in control subjects both in the ballooning and in the non-ballooning segments. The native and post-USPIO T2*

values in patients with takotsubo cardiomyopathy and matched control subjects are shown in Supplemental Table 2 and Supplemental Figure 1.

Myocardial Edema Assessed with Native T1 Mapping

In the scans performed during the acute phase, native T1 values were higher in patients with takotsubo cardiomyopathy in both ballooning and non-ballooning segments (p=<0.0001 for both, Table 2). At 5 months follow-up, T1 values were no longer different from controls in the ballooning (p=0.07) or in the non-ballooning segments (p=0.06).

Myocardial Energetics assessed with ^{31}P Cardiac Magnetic Resonance Spectroscopy

Resting cardiac energetic status (PCr/γATP ratio) was markedly reduced in patients with acute takotsubo cardiomyopathy compared to control subjects (p=<0.001) and this showed only partial recovery at follow-up (p=0.002; Table 2).

Systemic Inflammatory Cells and Monocyte Sub-population Phenotyping

Patients with acute takotsubo cardiomyopathy had a higher total white cell as well as neutrophil count at presentation compared to control subjects (p<0.001, Table 1). Although there was no difference in the total monocyte count, during the acute phase, patients with takotsubo cardiomyopathy had a higher percentage of classical $CD14^{++}CD16^{-}$ expressing monocytes (p=0.01), a lower percentage of intermediate $CD14^{++}CD16^{+}$ expressing monocytes (p=0.01) and a lower percentage of non-classical $CD14^{+}CD16^{++}$ expressing monocytes (p=0.006) compared to control subjects; (Table 3). When these acute post-takotsubo monocyte subpopulation responses were grouped by days 0-3, 4-7 and 8-12 post-acute event, it became evident that these changes were most pronounced on days 0-3 after presentation (Table 3, Figure 2). The greatest percentage increase in classical ($CD14^{++}CD16^{-}$) and greatest percentage decrease in intermediate ($CD14^{++}CD16^{+}$) and non-classical ($CD14^{+}CD16^{++}$) was found at this (days 0-3) time bracket. The percentages of classical ($CD14^{++}CD16^{-}$) and non-classical ($CD14^{+}CD16^{++}$) subpopulations became comparable to controls after 5 months, whereas the intermediate subset ($CD14^{++}CD16^{+}$) remained suppressed (p=0.01). *Ex vivo* culture of monocyte-derived macrophages demonstrated no functional difference in the dose-dependent USPIO uptake in cells sampled from patients with acute takotsubo cardiomyopathy when compared to those sampled from healthy control subjects (Supplemental Figure 2).

Serum cytokine profiles

Patients with acute takotsubo cardiomyopathy had higher serum concentrations of IL-6 and CXCL1 (GROα) chemokine compared to control subjects (p< 0.001 and p=0.01 respectively; Table 4). Although the concentrations of IL-6 fell at follow up compared to initial presentation, they remained elevated compared to control subjects (p=0.009). Apparent early increases in serum IL-8 concentrations in patients with takotsubo cardiomyopathy (p=0.07) became more pronounced by 5 months of follow-up (p=0.009).

Standard Cardiac Magnetic Resonance Imaging and Echocardiography

Consistent with previously reported findings[7,15,21], patients with takotsubo cardiomyopathy had alterations in left ventricular mass, ejection fraction and deformation analyses (Table 2). There were no significant correlations between acute-to-follow-up changes in any of the functional, structural or metabolic cardiac magnetic resonance parameters and either of the measured serum cytokines.

Symptoms and High Sensitivity Troponin at 5 Months Follow-up

At 5-month interview, 42% of patients reported ongoing symptoms. Of these, the majority (70%) of patients were NYHA Class I, 23% were NYHA Class II and 7% were NYHA Class III. Quality of life assessed with MLWHFQ showed a median score of 5 (range of 0-60 out of a maximum of 105) with a median physical domain score of 5 (range 0-30 out of a maximum of 40) and a median emotional domain score of 0 (range 0-17 out of a maximum of 25). The high sensitivity troponin at follow-up was 6.47 ± 0.6 ng/L.

Discussion

This is the first prospective evaluation of myocardial and systemic inflammation in acute and 5-month convalescent takotsubo cardiomyopathy. Using USPIO-enhanced magnetic resonance imaging, we demonstrate a macrophage-mediated cellular inflammatory response in the myocardium, superimposed on myocardial edema. Furthermore, we show systemic peripheral inflammatory responses, some of which appear to persist for at least 5 months. Taken together, our data demonstrate both localized and systemic inflammatory responses and uncover a previously unknown mechanistic pathway of takotsubo pathophysiology. These findings provide a potential explanation for the development of the long-term heart failure phenotype and poorer long-term prognosis, as well as suggesting that the acute inflammatory response could be a promising therapeutic target in this condition for which no effective treatment currently exists.

Our study has a number of important strengths. First, we conducted a multicentre study including patients with a clear and rigorously defined diagnosis of takotsubo cardiomyopathy (excluding any possibility of myocardial infarction or myocarditis), ensuring our findings are robust and generalizable. Second, we had a relatively large sample size and used a control population that was matched not only for age and sex but also for co-morbidities found in the study patients. Third, we undertook highly detailed and objective assessments of both myocardial and systemic inflammation using state-of-the art cardiac imaging including 24-hour post-USPIO-enhanced magnetic resonance imaging. This enabled us to assess tissue, cellular and humoral inflammation including myocardial tissue-resident macrophages.

Study rationale

The swift recovery of the left ventricular ejection fraction after an acute episode of takotsubo cardiomyopathy has misled clinicians to affirm that takotsubo is a rapidly resolving and self-limiting condition. In contrast to this assumption, two large registries reported that patients with takotsubo cardiomyopathy have a long-term prognosis comparable to patients with

myocardial infarction3,22. To provide a mechanistic explanation to these registry data, we have recently shown that patients who suffered a prior episode of takotsubo cardiomyopathy develop a long-term heart failure phenotype4. This, therefore, begs the question of what are the mechanistic processes that account for this evolution towards heart failure?

Myocardial edema, inflammation and energetic impairment

Previous reports, including our own work, have demonstrated that there is an unprecedented degree of myocardial edema in the myocardium of patients with acute takotsubo cardiomyopathy. Our current larger cohort confirms these findings of pan-left ventricular edema (high-native T1 values)5,23. However, the substrate for this widespread myocardial edema is so far un-explained. In the present study, we have gone on to show, for the first time, that USPIO-enhanced magnetic resonance imaging suggests a macrophage-driven cellular infiltration within the myocardium. As we and others have shown, the main cells capable of phagocytosing USPIO that accumulate in the infarcted myocardium are monocyte-derived macrophages12,13,24,25. Indeed, biopsies from patients with acute takotsubo cardiomyopathy have demonstrated the presence of macrophages albeit from the right ventricular myocardium26. We have recently reported post-mortem cases of takotsubo cardiomyopathy in which we observed clusters of macrophages (CD68^{+} staining) in the left ventricular myocardium of patients who died within 5 days of acute presentation; these were predominantly M1 macrophages, supporting the pro-inflammatory findings in the current study27. It is therefore most likely that the cellular protagonists responsible for the organ-specific inflammatory response observed herein (USPIO uptake in the myocardium) are macrophages. This is in contrast to other types of acute heart failure presentations, such as acute myocarditis, where our group have previously shown that USPIO-enhanced magnetic resonance imaging was not able to detect a myocardial macrophage infiltrate, as the inflammatory cells involved in acute myocarditis are predominantly lymphocytes28. Moreover, our *ex-vivo* macrophage culture data suggest that the increase in USPIO uptake in the myocardium of patients with takotsubo cardiomyopathy was not attributable to an increased efficiency of USPIO uptake but to a large increase in tissue-resident myocardial macrophages. This is also in keeping with the most accepted pathophysiological trigger of a catecholamine surge29, as catecholamines themselves can induce regional myocardial inflammation30, possibly enhanced in a susceptible population of women (who have a higher catecholamine sensitivity)31. Finally, we recapitulated the energetic impairment previously reported in a smaller cohort and its incomplete recovery during follow-up. Whether the inflammatory output and the energetic impairment are causally linked remains to be established.

Monocyte subpopulations behaviour in takotsubo cardiomyopathy

Here we describe for the first time that patients with takotsubo cardiomyopathy exhibit a substantial increase in the pro-inflammatory, classical monocyte subset (CD14^{++}CD16^{-}) at the expense of a decrease in the other two sub-populations: CD14^{++}CD16^{+} (intermediate) and CD14^{+}CD16^{++} (non-classical, patrolling and reparative). It is now recognized that the CD14^{++}CD16^{-} (classical) monocytes mature through a continuum to CD14^{++}CD16^{+} (intermediate) then CD14^{+}CD16^{++} (non-classical)32. We propose that the increased percentage of CD14^{++}CD16^{-} (classical) monocytes is due to an acute release of

CD14^{++}CD16$^-$ (classical) monocytes from the bone marrow (and spleen) into the circulation and/or the infiltration of CD14^{++}CD16$^+$ (intermediate) and CD14$^+$CD16^{++} (non-classical) monocytes into myocardial tissue. Such sequestration would decrease the overall percentages of the latter two subsets. It is likely that the phagocytosing macrophage infiltrate detected in the myocardium originates from the migration of these circulating monocytes into the heart, rather than proliferation of resident myocardial macrophages, as has been shown in experimental models following insult[33]. Perhaps the most interesting finding is that the intermediate monocyte subset (CD14^{++}CD16$^+$) remains low during follow-up, suggesting a lower degree of turnover. This is in complete contrast with patients who have sustained an acute myocardial infarction and experimental models of myocardial infarction where a two phase progression in monocyte activation has been defined: immediately after myocardial infarction, the classical, pro-inflammatory CD14^{++}CD16$^-$ subset is recruited whereas by day 7 post-myocardial infarction the non-classical CD14$^+$CD16^{++} subset becomes dominant, implying lesser pro-inflammatory response and tissue repair[34,35]. The decrease in percentage of the intermediate subset in patients with takotsubo cardiomyopathy may relate to the failure of their myocardial inflammation to resolve resulting in a low level chronic inflammatory state.

Systemic inflammatory response

The increase in systemic inflammatory cytokines/chemokines IL-6, IL-8 and CXCL1 (GROα) is in keeping with the increase in myocardial inflammation and increase in percentage of blood CD14^{++}CD16$^-$ monocytes, highlighting the inflammatory nature of the condition. The increase in IL-8 and CXCL1 (GROα) may relate to monocyte adhesion and macrophage infiltration into the myocardium or release of inflammatory cells from the bone marrow[36] while IL-6 is a robust pro-inflammatory marker.

Finally, almost half of the patients remained symptomatic at the time of follow-up. The high sensitivity cardiac troponin levels were above the 5 ng/mL threshold that defined populations at increased subsequent risk of cardiac events in patients suspected of acute coronary syndromes[37,38]. However, this finding will require validation in larger cohorts given the different pathophysiology of these conditions.

Study limitations

There is a number of limitations to the current study. Firstly, we did not obtain biopsies from ballooning or non-ballooning areas of the left ventricle in patients with takotsubo cardiomyopathy to demonstrate macrophage-USPIO co-localisation; myocardial biopsies would have implied a second invasive procedure during an acute illness combined with participation in a demanding research protocol in patients who experienced a stress-induced condition. However, our published data from post-mortem myocardium of patients with takotsubo cardiomyopathy demonstrates the clusters of macrophage infiltrates within the myocardium[27]. Second, we used T1 mapping for identification of edema instead of T2 mapping schemes and this allowed us to compare the current group with those from our previously published cohorts[5,15]. Both native and post-USPIO myocardial T2* values could be affected by concurrent myocardial pathology such as edema, haemorrhage, vasodilatation or different proportions of oxygenated or deoxygenated haemoglobin. We are unable to

either confirm or refute the possible contribution of some of these to the directly measured T2* values – which may explain some of the differences seen in either native or post-USPIO T2* values between groups (Supplementary Table 2). Therefore, we expressed the myocardial USPIO uptake as the change in T2* from the pre- (native) to post-USPIO images which were acquired only 24 hours apart. In this way, any contribution of any significant concurrent myocardial pathology should have been subtracted, logically assuming that the subtraction will eliminate the non-contrast agent effects. At the current time measurements of effect size between health and disease for both 3T scanners have not been computed and the majority of patients in this study were scanned in one centre. A final limitation is not being able to infer from our study whether inflammation is a cause or a consequence of the acute takotsubo event. Moreover, it is unclear whether this inflammation is maladaptive and implicated in the persistence in the long term consequences of this condition. This can only be addressed by randomised controlled trials of anti-inflammatory interventions.

Conclusions

We demonstrate for the first time that takotsubo cardiomyopathy is accompanied by myocardial and systemic inflammatory activation, with myocardial macrophage infiltration, and acute pro-inflammatory monocyte and cytokine activation. These changes evolve into a low-grade, chronic inflammatory state that remains detectable at least 5 months after acute presentation.

Supplementary Material

Refer to Web version on PubMed Central for supplementary material.

Acknowledgements

References

1. Redfors B, Vedad R, Angeras O, Ramunddal T, Petursson P, Haraldsson I, Ali A, Dworeck C, Odenstedt J, Ioaness D, Libungan B, et al. Mortality in takotsubo syndrome is similar to mortality in

myocardial infarction - A report from the SWEDEHEART registry. Int J Cardiol. 2015; 185:282–289. [PubMed: 25818540]

2. Brinjikji W, El-Sayed AM, Salka S. In-hospital mortality among patients with takotsubo cardiomyopathy: a study of the National Inpatient Sample 2008 to 2009. Am Heart J. 2012; 164:215–221. [PubMed: 22877807]

3. Tornvall P, Collste O, Ehrenborg E, Jarnbert-Petterson H. A Case-Control Study of Risk Markers and Mortality in Takotsubo Stress Cardiomyopathy. J Am Coll Cardiol. 2016; 67:1931–1936. [PubMed: 27102508]

4. Scally C, Rudd A, Mezincescu A, Wilson H, Srivanasan J, Horgan G, Broadhurst P, Newby DE, Henning A, Dawson DK. Persistent Long-Term Structural, Functional, and Metabolic Changes After Stress-Induced (Takotsubo) Cardiomyopathy. Circulation. 2018; 137:1039–1048. [PubMed: 29128863]

5. Dawson DK, Neil CJ, Henning A, Cameron D, Jagpal B, Bruce M, Horowitz J, Frenneaux MP. Tako-Tsubo Cardiomyopathy: A Heart Stressed Out of Energy? Jacc-Cardiovascular Imaging. 2015; 8:985–987. [PubMed: 25499134]

6. Scally C, Ahearn T, Rudd A, Neil CJ, Srivanasan J, Jagpal B, Horowitz J, Frenneaux M, Dawson DK. Right Ventricular Involvement and Recovery After Acute Stress-Induced (Tako-tsubo) Cardiomyopathy. Am J Cardiol. 2016; 117:775–780. [PubMed: 26782339]

7. Eitel I, Von Knobelsdorff-Brenkenhoff F, Bernhardt P, Carbone I, Muellerleile K, Aldrovandi A, Francone M, Desch S, Gutberlet M, Strohm O. Clinical characteristics and cardiovascular magnetic resonance findings in stress (takotsubo) cardiomyopathy. JAMA - Journal of the American Medical Association. 2011; 306:277–286. [PubMed: 21771988]

8. Neil CJ, Nguyen TH, Singh K, Raman B, Stansborough J, Dawson D, Frenneaux MP, Horowitz JD. Relation of delayed recovery of myocardial function after takotsubo cardiomyopathy to subsequent quality of life. Am J Cardiol. 2015; 115:1085–1089. [PubMed: 25724780]

9. Madhavan M, Prasad A. Proposed Mayo Clinic criteria for the diagnosis of Tako-Tsubo cardiomyopathy and long-term prognosis. Herz. 2010; 35:240–243. [PubMed: 20582391]

10. Lyon AR, Bossone E, Schneider B, Sechtem U, Citro R, Underwood SR, Sheppard MN, Figtree GA, Parodi G, Akashi YJ, Ruschitzka F, et al. Current state of knowledge on Takotsubo syndrome: a position statement from the task force on Takotsubo syndrome of the Heart Failure Association of the European Society of Cardiology. European Journal of Heart Failure. 2016; 18:8–27.

11. Ruehm SG, Corot C, Vogt P, Kolb S, Debatin JF. Magnetic Resonance Imaging of Atherosclerotic Plaque With Ultrasmall Superparamagnetic Particles of Iron Oxide in Hyperlipidemic Rabbits. Circulation. 2001; 103:415–422. [PubMed: 11157694]

12. Stirrat CG, Alam SR, MacGillivray TJ, Gray CD, Dweck MR, Raftis J, Jenkins WS, Wallace WA, Pessotto R, Lim KH, Mirsadraee S, et al. Ferumoxytol-enhanced magnetic resonance imaging assessing inflammation after myocardial infarction. Heart. 2017; 103:1528–1535. [PubMed: 28642288]

13. Yilmaz A, Dengler MA, van der Kuip H, Yildiz H, Rosch S, Klumpp S, Klingel K, Kandolf R, Helluy X, Hiller KH, Jakob PM, et al. Imaging of myocardial infarction using ultrasmall superparamagnetic iron oxide nanoparticles: a human study using a multi-parametric cardiovascular magnetic resonance imaging approach. Eur Heart J. 2013; 34:462–475. [PubMed: 23103659]

14. Abeles RD, McPhail MJ, Sowter D, Antoniades CG, Vergis N, Vijay GK, Xystrakis E, Khamri W, Shawcross DL, Ma Y, Wendon JA, et al. CD14, CD16 and HLA-DR reliably identifies human monocytes and their subsets in the context of pathologically reduced HLA-DR expression by CD14(hi) /CD16(neg) monocytes: Expansion of CD14(hi) /CD16(pos) and contraction of CD14(lo) /CD16(pos) monocytes in acute liver failure. Cytometry A. 2012; 81:823–834. [PubMed: 22837127]

15. Schwarz K, Ahearn TSC, Srinivasan J, Neil C, Rudd A, Jagpal B, Frenneaux M, Pislaru C, Horowitz J, Dawson DK. Alterations in Cardiac Deformation, Timing of Contraction and Relaxation and Early Myocardial Fibrosis Accompany the Apparent Recovery of Acute Stress-Induced (Takotsubo) Cardiomyopathy: an End to the Concept of Transience. Journal Am Soc Echo. 2017; 8:745–755.

16. Neubauer S, Horn M, Naumann A, Tian R, Hu K, Laser M, Friedrich J, Gaudron P, Schnackerz K, Ingwall JS. Impairment of energy metabolism in intact residual myocardium of rat hearts with chronic myocardial infarction. J Clin Invest. 1995; 95:1092–1100. [PubMed: 7883957]

17. Shivu GN, Abozguia K, Phan TT, Ahmed I, Henning A, Frenneaux M. (31)P magnetic resonance spectroscopy to measure in vivo cardiac energetics in normal myocardium and hypertrophic cardiomyopathy: Experiences at 3T. Eur J Radiol. 2010; 73:255–259. [PubMed: 19056193]

18. Bottomley PA, Hardy CJ, Weiss Robert G. Correcting human heart 31P NMR spectra for partial saturation. Evidence that saturation factors for PCr/ATP are homogeneous in normal and disease states. Journal of Magnetic Resonance Imaging. 1991; 95:341–355.

19. Conway MA, Bottomley PA, Ouwerkerk R, Radda GK, Rajagopalan B. Mitral Regurgitation: Impaired Systolic Function, Eccentric Hypertrophy, and Increased Severity Are Linked to Lower Phosphocreatine/ATP Ratios in Humans. Circulation. 1998; 97:1716–1723. [PubMed: 9591766]

20. Cerqueira MD, Weissman NJ, Dilsizian V, Jacobs AK, Kaul S, Laskey WK, Pennell DJ, Rumberger JA, Ryan T, Verani MS. Standardized myocardial segmentation and nomenclature for tomographic imaging of the heart: a statement for healthcare professionals from the Cardiac Imaging Committee of the Council on Clinical Cardiology of the American Heart Association. Circulation. 2002; 105:539–542. [PubMed: 11815441]

21. Ono R, Falcão LM. Takotsubo cardiomyopathy systematic review: Pathophysiologic process, clinical presentation and diagnostic approach to Takotsubo cardiomyopathy. Int J Cardiol. 2016; 209:196–205. [PubMed: 26896623]

22. Templin C, Ghadri JR, Diekmann J, Napp LC, Bataiosu DR, Jaguszewski M, Cammann VL, Sarcon A, Geyer V, Neumann CA, Seifert B, et al. Clinical Features and Outcomes of Takotsubo (Stress) Cardiomyopathy. N Engl J Med. 2015; 373:929–938. [PubMed: 26332547]

23. Neil C, Nguyen TH, Kucia A, Crouch B, Sverdlov A, Chirkov Y, Mahadavan G, Selvanayagam J, Dawson D, Beltrame J, Zeitz C, et al. Slowly resolving global myocardial inflammation/oedema in Tako-Tsubo cardiomyopathy: evidence from T2-weighted cardiac MRI. Heart. 2012; 98:1278–1284. [PubMed: 22791656]

24. Alam SR, Shah ASV, Richards J, Lang NN, Barnes G, Joshi N, MacGillivray T, McKillop G, Mirsadraee S, Payne J, Fox KAA, et al. Ultrasmall Superparamagnetic Particles of Iron Oxide in Patients With Acute Myocardial Infarction: Early Clinical Experience. Circ Cardiovasc Imaging. 2012; 5:559–565. [PubMed: 22875883]

25. Bietenbeck M, Florian A, Sechtem U, Yilmaz A. The diagnostic value of iron oxide nanoparticles for imaging of myocardial inflammation--quo vadis? J Cardiovasc Magn Reson. 2015; 17:54. [PubMed: 26152269]

26. Nef HM, Möllmann H, Kostin S, Troidl C, Voss S, Weber M, Dill T, Rolf A, Brandt R, Hamm CW, Elsässer A. Tako-Tsubo cardiomyopathy: intraindividual structural analysis in the acute phase and after functional recovery. Eur Heart J. 2007; 28:2456–2464. [PubMed: 17395683]

27. Wilson H, Cheyne L, Brown P, Kerr K, Hannah A, Srinivasan J, Duniak N, Horgan G, Dawson D. Characterization of the Myocardial Inflammatory Response in Acute Stress-Induced (Tako-tsubo-like) Cardiomyopathy. J Am Coll Cardiol Basic Transl Sci. 2018; doi: 10.1016/j.jacbts. 2018.08.006

28. Stirrat CG, Alam SR, MacGillivray TJ, Gray CD, Dweck MR, Dibb K, Spath N, Payne JR, Prasad SK, Gardner RS, Mirsadraee S, et al. Ferumoxytol-enhanced magnetic resonance imaging in acute myocarditis. Heart. 2018; 104:300–305. [PubMed: 28986407]

29. Pelliccia F, Kaski JC, Crea F, Camici PG. Pathophysiology of Takotsubo Syndrome. Circulation. 2017; 135:2426–2441. [PubMed: 28606950]

30. Roghi A, Pedrotti P, Milazzo A, Bonacina E, Bucciarelli-Ducci C. Adrenergic myocarditis in pheochromocytoma. J Cardiovasc Magn Reson. 2011; 13:4. [PubMed: 21223554]

31. Friedrich MG, Cocker MS. Stress-induced cardiomyopathy: a syndrome of the susceptible patient? Expert Rev Cardiovasc Ther. 2012; 10:271–273. [PubMed: 22390796]

32. Patel AA, Zhang Y, Fullerton JN, Boelen L, Rongvaux A, Maini AA, Bigley V, Flavell RA, Gilroy DW, Asquith B, Macallan D, et al. The fate and lifespan of human monocyte subsets in steady state and systemic inflammation. J Exp Med. 2017; 214:1913–1923. [PubMed: 28606987]

33. Mylonas KJ, Jenkins SJ, Castellan RF, Ruckerl D, McGregor K, Phythian-Adams AT, Hewitson JP, Campbell SM, MacDonald AS, Allen JE, Gray GA. The adult murine heart has a sparse, phagocytically active macrophage population that expands through monocyte recruitment and adopts an 'M2' phenotype in response to Th2 immunologic challenge. Immunobiology. 2015; 220:924–933. [PubMed: 25700973]

34. Nahrendorf M, Swirski FK. Monocyte and Macrophage Heterogeneity in the Heart. Circ Res. 2013; 112:1624–1633. [PubMed: 23743228]

35. Nahrendorf M, Pittet MJ, Swirski FK. Monocytes: Protagonists of Infarct Inflammation and Repair After Myocardial Infarction. Circulation. 2010; 121:2437–2445. [PubMed: 20530020]

36. Papadopoulou C, Corrigall V, Taylor PR, Poston RN. The role of the chemokines MCP-1, GRO-alpha, IL-8 and their receptors in the adhesion of monocytic cells to human atherosclerotic plaques. Cytokine. 2008; 43:181–186. [PubMed: 18579408]

37. Chapman AR, Lee KK, McAllister DA, Cullen L, Greenslade JH, Parsonage W, Worster A, Kavsak PA, Blankenberg S, Neumann J, Sorensen NA, et al. Association of High-Sensitivity Cardiac Troponin I Concentration With Cardiac Outcomes in Patients With Suspected Acute Coronary Syndrome. JAMA. 2017; 318:1913–1924. [PubMed: 29127948]

38. Shah AS, Anand A, Sandoval Y, Lee KK, Smith SW, Adamson PD, Chapman AR, Langdon T, Sandeman D, Vaswani A, Strachan FE, et al. High-sensitivity cardiac troponin I at presentation in patients with suspected acute coronary syndrome: a cohort study. Lancet. 2015; 386:2481–2488. [PubMed: 26454362]

Clinical Perspective

What is new?

- Patients with acute takotsubo cardiomyopathy have macrophage-mediated myocardial inflammation

- Patients with acute takotsubo cardiomyopathy demonstrate modulation of peripheral monocyte subsets and increased systemic pro-inflammatory cytokines

- Systemic inflammation persists for at least 5 months

What are the clinical implications?

- These findings further elucidate the mechanisms and pathogenesis of takotsubo cardiomyopathy

- Systemic and myocardial inflammation may serve as a therapeutic target for patients with acute takotsubo cardiomyopathy
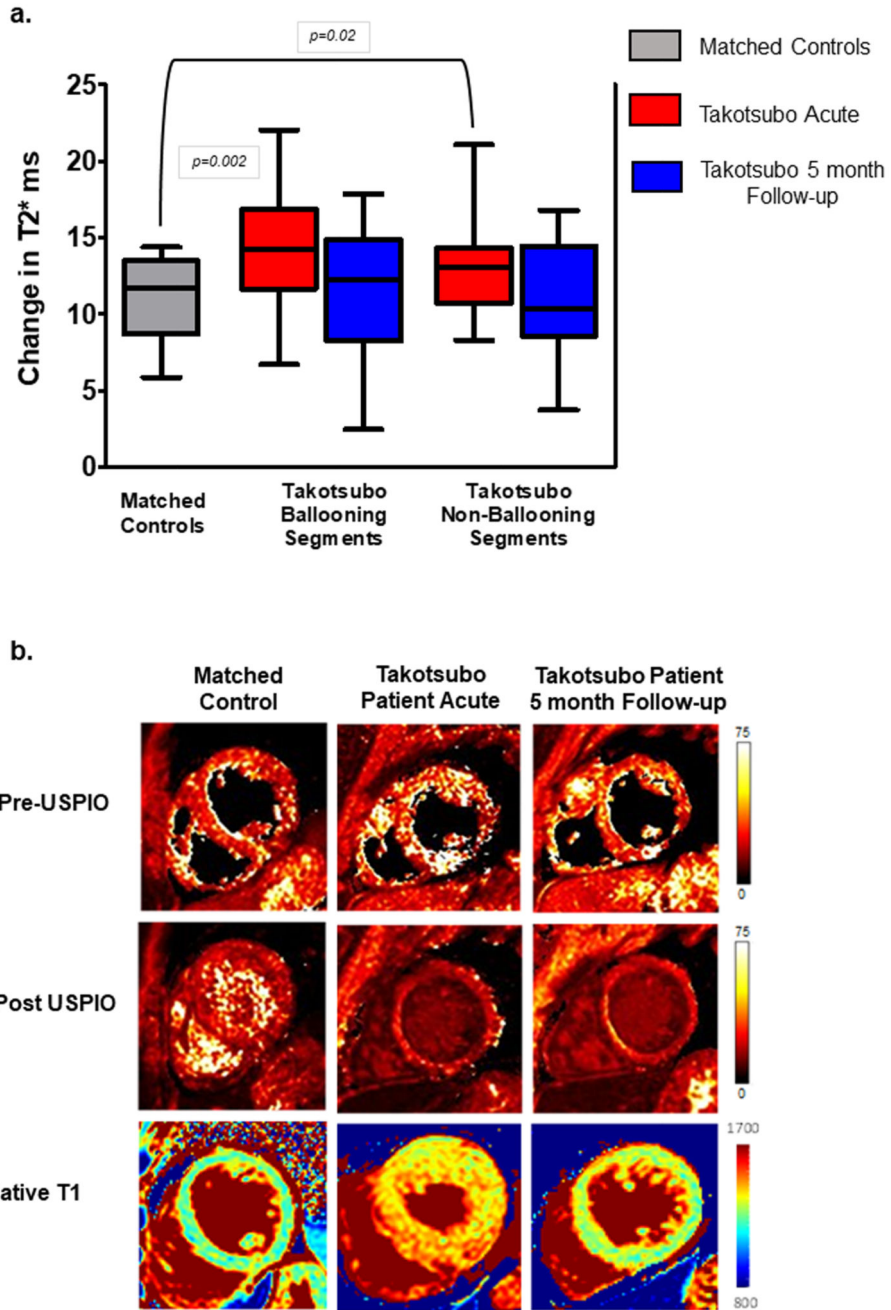
Figure 1.
Ultrasmall superparamagnetic iron oxide particles (USPIO) uptake in to the myocardium in ballooning and non-ballooning segments versus matched controls as shown by change in T2*: a- at acute presentation and at follow-up. Data shown as median, 25th and 75th centiles and maximum and minimum (whiskers). b- Example of T2* maps before and after USPIO administration and native T1 maps in a control subject compared with a patient with takotsubo cardiomyopathy at presentation and at follow-up.
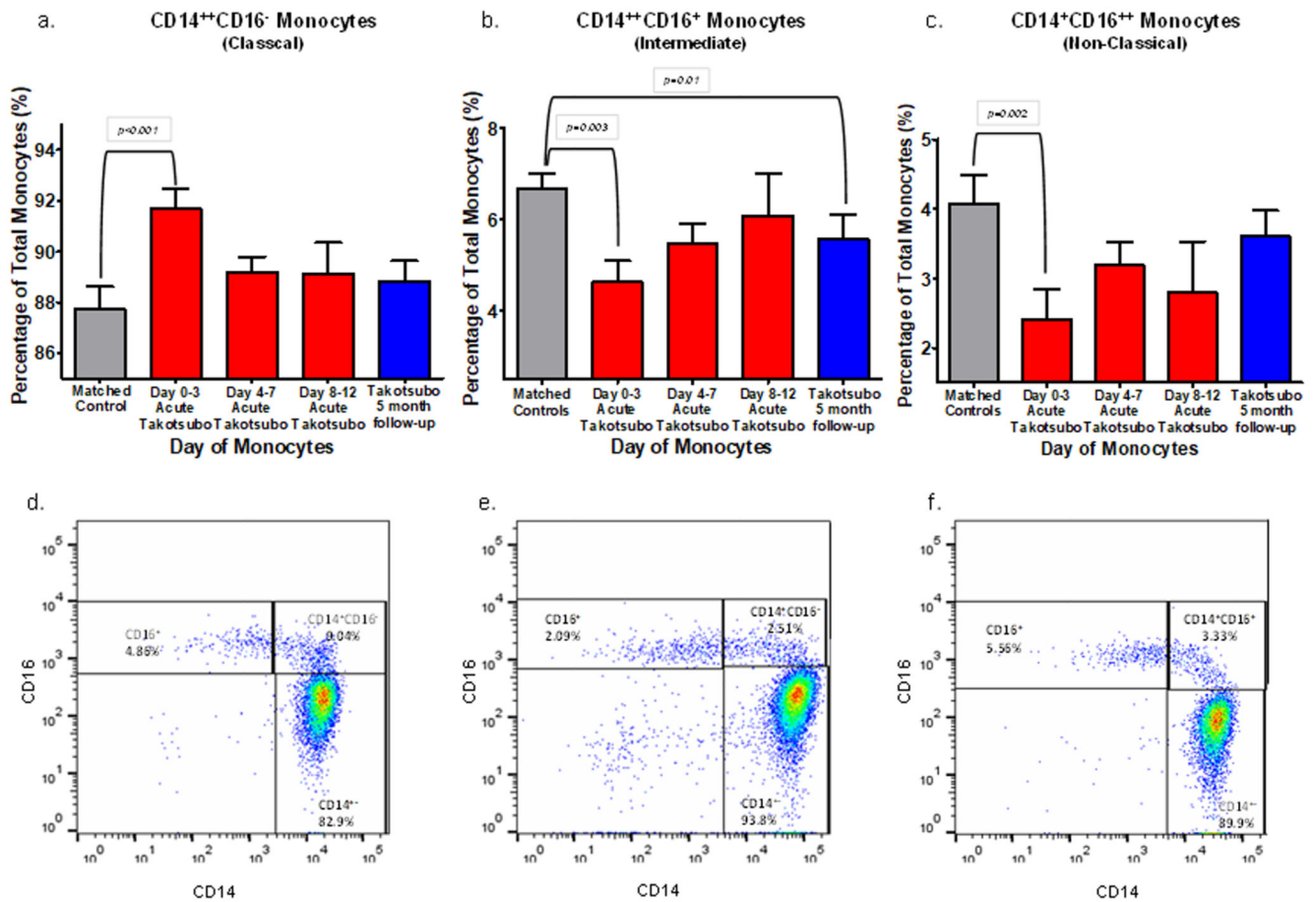
Figure 2.
Top: The dynamic of each monocyte sub-population in takotsubo patients compared to matched controls: the CD14^{++}CD16$^-$ (classical, pro-inflammatory), CD14^{++}CD16$^+$ (intermediate) and CD14$^+$CD16^{++} (non-classical) monocyte sub-populations analysed at specific time points after acute presentation in takotsubo patients compared to matched controls (a-c), data is shown as mean±SEM (standard error of the mean). Bottom: Representative examples of CD14/CD16 bi-variate plots in: d - matched control, e - acute-phase takotsubo (sampled on day 2), and f - takotsubo 5 months follow-up.

Table 1

Characteristics of study population

BMI, Body max index; BNP, brain natriuretic peptide, ECG, electrocardiogram; MLWHFQ, Minnesota living with heart failure questionnaire; LBBB, left bundle branch block; LV, left ventricular; WCC, white cell count. Data shown as mean±SEM (standard error of the mean) unless otherwise stated.

	Patients with Takotsubo Cardiomyopathy n=55	Control Subjects n=51	p value
Female (%)	50 (91)	46 (90)	0.93
Age, years, median (range)	64 (28-83)	64 (38-85)	0.94
BMI, kg/m^2	26±0.81	26±0.51	0.71
Past Medical History n (%)			
Hypertension	15(27)	13(25)	0.79
Diabetes	7(12)	5(10)	0.38
Psychiatric Disease	11(20)	0	
Depression	7(13)	0	
Anxiety	4(7)	0	
Paroxysmal Atrial Fibrillation	5(9)	0	
Presenting symptom n (%)			
Chest Pain	46(84)	-	
Breathlessness	3(5)	-	
Syncope	0	-	
Other	6(11)	-	
LV ballooning type, n (%)			
Apical	48(87)	-	
Mid-cavity	4(7)	-	
Basal	3(6)		
Presenting ECG, n (%)			
ST elevation	23(42)	-	
Non-ST elevation	24(44)	-	
LBBB	2(4)	-	
Other	6(10)		
Stressor, n (%)			
Physical	18(33)	-	
Emotional	27(49)	-	
None	10(18)	-	
Bloods at presentation (upper limit of reference range)			
Troponin I, ng/l (40)	4393±742	-	
BNP, pg/ml (100pg/ml)	297±65	32.7±4.6	**0.002**
WCC, x10^9/l (10 x10^9/l)	10.4±0.33	5.6±0.30	**<0.001**
Neutrophils x10^9/l (7 x10^9/l)	7.9±0.35	3.1±0.20	**<0.001**
Eosinophils x10^9/l (0.5 x10^9/l)	0.15±0.14	0.19±0.09	0.46
Basophils x10^9/ l(0.1x10^9/l)	0.04±0.02	0.04±0.02	0.94

	Patients with Takotsubo Cardiomyopathy n=55	Control Subjects n=51	p value
Lymphocytes x10^9/ l(4 x10^9/l)	1.72±0.89	1.74±0.38	0.93
Monocytes x10^9/l (0.8x10^9/l)	0.49±0.21	0.45±0.21	0.38
MLWHFQ score at follow-up median (range)			
Total score (out of 105)	5 (0-60)	-	
Physical domain (out of 40)	5 (0-30)	-	
Emotional domain (out of 25)	0 (0-17)	-	
BNP at follow-up, pg/ml (35 pg/ml)	77.9±45	32.7±4.6	**0.003**

Table 2

Magnetic resonance imaging and echocardiography findings

Imaging data for Takotsubo patients at acute presentation and at follow-up compared to controls. USPIO, ultra-small superparamagnetic particles of iron oxide; PCr/γATP, phosphocreatine/γ adenosine triphosphate; LV, left ventricle; LVEDV, left ventricular end-diastolic volume; LVESV, left ventricular end-systolic volume; EF, Ejection Fraction; RVSP, Right ventricular systolic pressure.

†**PCr/γATP** performed only in patients scanned in Aberdeen, n=48

p values for comparisons were calculated using *t*-tests with degrees of freedom estimated by the Satterthwaite method (degrees of freedom for change in T2*=37-65)

	Patients with Takotsubo Cardiomyopathy (Acute) n=55	Patients with Takotsubo Cardiomyopathy (5 Months) n=48	Matched control subjects n=51	p value Acute vs Control	p value 5 Months vs Control	p value Acute vs 5-Month Follow-up
Change in T2* post USPIO (ms)						
Ballooning Segments	14.3±0.65	11.9±0.84	10.5±0.98	**0.002**	0.28	**0.02**
Non-Ballooning Segments	12.9±0.54	11.6±0.65	10.6±0.83	**0.02**	0.32	0.08
Whole left ventricle	13.3±0.44	11.4±0.54	10.9±0.73	**0.006**	0.62	**0.002**
Basal	12.1±0.59	11.3±0.73	10.9±0.94	0.33	0.73	0.39
Mid-cavity	13.8±0.50	11.3±0.62	11.2±0.83	**0.009**	0.94	**0.001**
Apical	14.4±0.71	11.7±0.88	10.4±1.14	**0.004**	0.38	**0.01**
Native T1 (ms)						
Ballooning Segments	1417±11.82	1257±18.24	1215±17.44	**<0.0001**	0.07	**<0.0001**
Non-Ballooning Segments	1329±8.03	1245±10.72	1213±12.07	**<0.0001**	0.06	**<0.0001**
Whole left ventricle	1358±9.88	1245±13.41	1204±14.98	**<0.0001**	**0.03**	**<0.0001**
Basal	1311±8.70	1243±12.26	1237±13.34	**<0.0001**	0.68	**<0.0001**
Mid-cavity	1358±9.71	1246±14.79	1214±16.24	**<0.0001**	0.14	**<0.0001**
Apical	1398±14.04	1252±18.79	1194±20.43	**<0.0001**	0.06	**<0.0001**
PCr/γATP †	1.25±0.10	1.4±0.12	1.9±0.11	**<0.001**	**0.002**	0.43
LVEDV index, ml/m²	73±1.99	71±2.56	72±2.72	0.72	0.63	0.34
LVESV index, ml/m²	30±1.43	24±1.88	26±1.94	0.13	0.53	**0.001**
LV mass index, g/m²	77±1.73	63±2.35	64±2.30	**<0.001**	0.68	**<0.001**
LV EF, %	59±1.23	67±1.72	64±1.56	**0.01**	0.22	**<0.001**
Echocardiography						

	Patients with Takotsubo Cardiomyopathy (Acute) n=55	Patients with Takotsubo Cardiomyopathy (5 Months) n=48	Matched control subjects n=51	p value Acute vs Control	p value 5 Months vs Control	p value Acute vs 5-Month Follow-up
EF, %	54±1.52	64±2.08	64±2.02	<0.001	0.88	<0.001
Estimated RVSP, mmHg	29±2.44	31±2.91	27±0.98	0.32	0.09	0.54
Global longitudinal strain, %	-12.4±0.51	-18.8±0.72	-19.7±0.78	<0.001	0.48	<0.001
Apical circumferential strain, %	-13.0±0.84	-19.4±1.12	-23.4±1.04	<0.001	0.01	<0.001
LV twist, °	11.9±1.12	13.4±1.64	23.3±1.49	<0.001	<0.001	0.48
LV twist rate, °/s	82.1±5.14	95.0±6.69	114.7±6.22	<0.001	0.03	0.14
LV untwist rate, °/s	-60±7.89	-91±11.21	-112±10.04	<0.01	0.23	0.02

Table 3

Monocyte profile in patients with takotsubo cardiomyopathy and matched control subjects

Monocyte sub-populations in takotsubo patients acutely, at follow up and in matched controls. Data shown as mean±SEM (standard error of the mean).

p values for comparisons were calculated using *t*-tests with degrees of freedom estimated by the Satterthwaite method (degrees of freedom for CD14++CD16- were 64-87, for CD14++16+ were 60-87 and for CD14+CD16++ were 65-87)

Sub-populations of monocytes	Patients with Takotsubo Cardiomyopathy (Acute) n=55	Patients with Takotsubo Cardiomyopathy (5 Months) n=48	Matched control subjects n=51	P value Acute vs Control	P value 5 Months vs Control	p value Acute vs 5-Month Follow-up
All days						
CD14++CD16- (%)	90.0±0.54	88.8±0.64	87.1±0.94	**0.01**	0.20	0.09
CD14++16+ (%)	5.4±0.34	5.5±0.41	6.9±0.61	**0.01**	**0.01**	0.78
CD14+CD16++ (%)	2.7±0.26	3.6±0.33	4.2±0.48	**0.006**	0.34	**0.03**
Day 0-3						
CD14++CD16- (%)	91.7±0.93	88.8±0.64	87.1±0.94	**0.001**	0.20	**0.008**
CD14++16+ (%)	4.7±0.58	5.5±0.41	6.9±0.61	**0.003**	**0.01**	0.21
CD14+CD16++ (%)	2.4±0.47	3.6±0.33	4.2±0.48	**0.002**	0.34	**0.01**
Day 4-7						
CD14++CD16- (%)	88.7±0.89	88.8±0.64	87.1±0.94	0.14	0.20	0.72
CD14++16+ (%)	5.6±0.56	5.5±0.41	6.9±0.61	0.12	**0.01**	0.48
CD14+CD16++ (%)	3.0±0.44	3.6±0.33	4.2±0.48	0.12	0.34	0.58
Day 8-12						
CD14++CD16- (%)	89.3±1.19	88.8±0.64	87.1±0.94	0.17	0.20	0.73
CD14++16+ (%)	6.0±0.74	5.5±0.41	6.9±0.61	0.36	**0.01**	0.41
CD14+CD16++ (%)	2.8±0.59	3.6±0.33	4.2±0.48	**0.03**	0.34	0.22

Table 4

Serum cytokine concentrations in patients with takotsubo cardiomyopathy and matched control subjects

Serum cytokine concentrations in patients with takotsubo cardiomyopathy acutely and at follow up, and in matched control subjects. Interleukins (IL-1βIL-6, IL-8(CXCL8), IL-10, IL-12p40); MCP-1, Monocyte chemoattractant protein 1; CXCL1 chemokine (C-X-C motif) ligand 1 or growth regulated protein (GROα); TNF-α, tumour necrosis factor alpha; IFN-γ, interferon gamma. All data shown as mean±SEM (standard error of the mean). p values for comparisons were calculated using t-tests with degrees of freedom estimated by the Satterthwaite method (degrees of freedom for IL-6 were 11-80)

	Patients with Takotsubo Cardiomyopathy (Acute) n=55	Patients with Takotsubo Cardiomyopathy (5 Months) n=48	Matched control subjects n=51	P value Acute vs Control	P value 5 Months vs Control	p value Acute vs 5-Month Follow-up
IL-1β (pg/ml)	4.2±2.31	3.9±2.36	7.7±2.64	0.32	0.34	0.81
IL-6 (pg/ml)	23.1±4.54	18.3±5.17	6.5±5.83	**<0.001**	**0.008**	**0.01**
IL-8 (CXCL8) (pg/ml)	45.5±8.62	61.9±10.28	21.7±10.86	0.07	**0.009**	0.24
IL-10 (pg/ml)	6.3±1.10	5.2±1.34	5.7±1.27	0.83	0.78	0.47
IL-12p40 (pg/ml)	10.2±6.24	16.9±7.72	8.1±6.01	0.82	0.43	0.51
MCP-1 (pg/ml)	483±38.37	435±50.43	575±42.07	0.14	**0.03**	0.41
CXCL1 (GROα) (pg/ml)	1903±168.43	1650±214.02	1272±176.56	**0.01**	0.15	0.34
TNFα (pg/ml)	12.5±1.47	12.8±1.82	12.4±1.89	0.89	0.90	0.86
IFNγ (pg/ml)	53.1±13.89	46.9±16.63	31.8±14.81	0.34	0.48	0.67